Adsorption of BTEX, MTBE and TAME on natural and modified diatomite

Maria Aivalioti *, Panagiotis Papoulias, Athanasia Kousaiti, Evangelos Gidarakos

Technical University of Crete, Department of Environmental Engineering, Laboratory of Toxic and Hazardous Waste Management, University Campus, P.C. 73100, Chania, Crete, Greece

A B S T R A C T

The removal of BTEX (benzene, toluene, ethyl-benzene and m-,p-,o-xylenes), MTBE (methyl tertiary butyl ether) and TAME (tertiary amyl methyl ether) from aqueous solutions by raw, thermally, chemically and both chemically and thermally treated diatomite was studied, through batch adsorption experiments. In total, 14 different diatomite samples were created and tested. Selected physical characteristics of the adsorbents, such as specific surface area and pore volume distribution, were determined. Matrix and competitive adsorption effects were also explored. It was proved that the diatomite samples were effective in removing BTEX, MTBE and TAME from aqueous solutions, with the sample treated with HCl being the most effective, as far as its adsorption capacity and equilibrium time are concerned. Among the contaminants, BTEX appeared to have the strongest affinity, based on mass uptake by the diatomite samples. Matrix effects were proved to be strong, significantly decreasing the adsorption of the contaminants onto diatomite. The kinetics data proved a closer fit to the pseudo second order model, while the isotherm experimental data were a better fit to the Freundlich model. However, the latter produced values of the isotherm constant $1/n$ greater than one, indicating unfavorable adsorption.

© 2011 Elsevier B.V. All rights reserved.

1. Introduction

Gasoline spills from leaking storage tanks and transfer pipes represent very common sources of soil, and consequently groundwater, contamination. Some of the most typical groundwater contaminants present in such events are BTEX (benzene-toluene-ethyl-benzene and xylenes), MTBE (methyl tertiary butyl ether) and TAME (tert-amyl methyl ether), which are considered to have several health side effects to humans, due to their toxic and/or carcinogenic properties.

Adsorption is a process that can be successfully applied for the removal of these contaminants, either in situ (in permeable reactive barriers) or ex-situ (in combination with pump-and-treat systems). It is relatively simple and can achieve high removal efficiencies. In the literature, BTEX removal from water by adsorption on resins [1], surfactant modified zeolites [2], organo-clays [3] and carbon nanotubes [4,5] seems to be an interesting perspective. Moreover, porous polymeric adsorbents [6], silicalite, mordenite, zeolite-β [7], as well as polymer [8], synthetic [9], carbonaceous [10] and solvent impregnated [11] resins and high silica [12,13], granular [14] and silicate-1/fly ash cenosphere (S/FAC) [15] zeolites have also been successfully tested for the removal of MTBE from water. For TAME adsorption, only bituminous-coal activated

carbon [16] and commercial activated carbon [17] have been used thus far.

Given the constant need to identify new, preferably more natural, more abundant and cheaper materials to replace activated carbon and/or other efficient, but still expensive, adsorbents, in this study, diatomite was tested for its adsorption potential for BTEX, MTBE and TAME from aqueous solutions.

Diatomite, also known as diatomaceous earth or kieselguhr, is a fine sedimentary rock of biogenetic origin, which mainly consists of amorphous hydrous silica ($SiO_2 \cdot nH_2O$) that derives from the skeletons of aquatic plants called diatoms. In addition to bound water, varying between 3.5 and 8%, the siliceous skeleton may also contain, in solid solution or as part of the SiO_2 complex, small amounts of associated inorganic components – alumina, principally – and lesser amounts of iron, alkaline earth, alkali metals and other minor constituents [18].

Diatomite is abundant in many areas of the world and has favorable physical characteristics, such as high porosity (25–65%) [19,20], small particle size, low thermal conductivity and density [21], large surface area [22] and high adsorption capacity [18,23]. The reactivity of diatomite is intrinsically linked to the presence of reactive sites on its surface, conditioning the charge, acidity, solubility and hydrophobicity of the surface and therefore governing the properties of related diatomite products to a great extent. The primary reactive sites on the surface of amorphous silica are the hydroxyl groups, while acid sites have also been considered to be important surface sites of diatomite [24].

---

* Corresponding author. Tel.: +30 28210 37790; fax: +30 28210 37850.
E-mail address: maivalioti@isc.tuc.gr (M. Aivalioti).

Nomenclature

q_e moles of adsorbate adsorbed at equilibrium per mass of adsorbent ($mmol\,g^{-1}$)

q_t moles of adsorbate adsorbed at time t per mass of adsorbent ($mmol\,g^{-1}$)

C_t concentration of adsorbate in the aqueous phase at equilibrium ($mmol\,L^{-1}$)

t adsorption time (h)

k_1 pseudo-first order rate constant (h^{-1})

k_2 pseudo-second order rate constant ($g\,mmol^{-1}\,h^{-1}$)

k_p diffusion rate constant ($mmol\,g^{-1}\,h^{-0.5}$)

x_i intraparticle diffusion model constant ($mmol\,g^{-1}$)

k_F Freundlich isotherm constant (related to the maximum adsorption capacity) ($mmol\,g^{-1}\,(L\,mmol^{-1})^{-1/n}$)

$1/n$ Freundlich isotherm constant that provides an indication of how favorable the adsorption process is

---

Diatomite has already been used for the adsorption of different elements and substances from water and wastewaters, either in its natural form (raw) or modified (chemically or thermally) – as already summarized in a previous study [25]. Such works have presented positive and promising results.

Thermal treatment is expected to cause physical desorption of the adsorbed water, which is partially structurally connected to the crystal mesh of the diatomite (forming active hydroxyl groups on it) [24], increasing the amount of exposed silanols [26] and resulting in a more hydrophobic diatomite surface [27]. Generally, an increase in thermal treatment has a prominent effect on the type, distribution and content of surface hydrated species (water, H-bonded silanols and isolated silanols), influencing key reactive sites for various surface reactions, including adsorption [26]. Thermal treatment may also cause the removal of volatile and organic admixtures.

Chemical treatment is a common procedure for the purification of diatomite and the modification of its surface properties for various purposes [28]. Typically, acid activators including sulfuric acid, hydrochloric acid, phosphorous acid and nitric acid and also alkaline activators including sodium hydroxide, sodium carbonate and potassium hydroxide are used for the purification of diatomite, removing residues and chemically creating finer pores [29]. Acid treatment reduces or eliminates all other oxides of diatomite relative to SiO_2 [30] and may generally result in an increase in its surface area and its adsorption capacity, as in any other clay mineral [29]. Alkaline agents such as sodium hydroxide are used to create more open pores, thus resulting in a larger surface area and total pore volume [29] by removing impurities and organic compounds [31].

Huttenloch et al. first examined the sorption of non-polar aromatic contaminants (o-xylene, toluene) by chlorosilane surface modified diatomite [32]; a promising but quite expensive adsorbent, due to the high cost of chlorosilanes. The capacity of raw and thermally treated diatomite to adsorb specific gasoline contaminants, such as BTEX and MTBE, was first explored by Aivalioti et al. [25] and thus far remains the only study of its kind.

In this paper, a commercial product of diatomite is examined for its adsorption capacity for BTEX and MTBE but also for TAME. In addition to its raw and thermally modified forms, several other forms – modified chemically and both chemically and thermally – are created and tested. Potential matrix and competitive effects on the adsorption efficiency are also explored.

2. Materials and methods

2.1. Adsorbent

The diatomite sample used in this study was a commercial product originating from Spain. Its chemical composition, using X-ray fluorescence (XRF) spectroscopy, was determined to be 89% SiO_2, 3% Al_2O_3, 1.4% K_2O, 1.4% Na_2O, 1% Fe_2O_3, 0.7% MgO, 0.4% CaO, and 0.2% TiO_2, while the main constituent minerals were quartz, illite, aragonite and calcite, as determined through X-ray diffraction (XRD).

The diatomite sample obtained was dried in an oven at 105 °C for 12 h and stored in closed plastic containers for further use.

During the experimental procedure, 14 different diatomite samples (Table 1) were created and tested in total. Thermal treatment was carried out at different temperatures in ambient air for 2 h. Chemical treatment was carried out using two different acids (HCl and H_2SO_4, 2.5 M each) and/or a strong base (NaOH 3 M). Diatomite was mixed with the acids at a solid (g)/liquid (mL) ratio of 1:20, then agitated for 3 h and finally filtered and washed with deionized water several times until the pH of the filtrate and the deionized water was the same. Diatomite was mixed with the base also at a solid (g)/liquid (mL) ratio of 1:20, then stirred for 3 h at 90 °C and finally filtered and washed with deionized water several times, as previously.

Small quantities (~1–2 g) of these samples were used to determine their surface area, mean pore size and pore volume distribution using the Nitrogen Gas Adsorption Method and a Nova 2200 Quanta Chrome analyzer. Also, for selected diatomite samples, new XRD analysis was carried out and scanning electron microscopy images were taken.

2.2. Adsorbate solutions

The chemicals tested in this study were benzene (Riedel-de Haen, purity: 99.7%), toluene (Riedel-de Haen, purity: 99.7%), ethyl benzene (Fluka, purity: 99%), m-xylene (Fluka, purity 99%), p-xylene (Fluka, purity 99%), o-xylene (Fluka, purity 99%), methyl tertiary butyl ether (Riedel-de Haen, purity: 99%) and tert-amyl methyl ether (Supelco, purity: 99%).

A stock solution in methanol (Sigma–Aldrich, puriss p.a. >99.8%-GC) was prepared in 25 mL glass volumetric flasks containing 2000 ppm from each of the above-mentioned contaminants, using glass gastight microliter syringes. The stock solution was transferred in a 22 mL glass vial, with a plastic screw cap and PTFE/silicone septum, sealed with Parafilm, without headspace, stored at 4 °C in the dark and used within a 1-month period for the daily creation of water solutions containing 5 ppm from each of the contaminants. These water solutions were used in both kinetic and isotherm experiments.

Ultrapure water was used from a Barnstead EASYpure II RF/UV water purification system.

2.3. Kinetic batch experiments

Kinetic experiments were carried out in 40 mL glass vials with gas-tight caps, non-permeable by organic vapors. Each vial contained 2 g of adsorbent. Head space within each vial was minimized (to exclude any contaminant volatilization phenomena), while agitation was applied at 20 °C. In each of the test vials of the diatomite samples, the contact time of the adsorbate and the adsorbent varied, with a maximum duration of 48 h. The solution samples were then filtered (0.45 μm pore filter) and analyzed. Each experiment was carried out at least twice and included a blank sample, in order to determine and take into account any potential contaminant losses due to volatilization. In any case, contaminant losses due to volatilization were determined to be lower than 13%.

Table 1
Diatomite samples.

Sample No.	Treatment	Identification
1	None	D_{raw}
2	Heating at 250 °C for 2 h	D_{250}
3	Heating at 350 °C for 2 h	D_{350}
4	Heating at 550 °C for 2 h	D_{550}
5	Heating at 750 °C for 2 h	D_{750}
6	Heating at 1.150 °C for 2 h	$D_{1.150}$
7	Agitation with HCl 2.5 M for 3 h, washing	D_{HCl}
8	Agitation with H_2SO_4 2.5 M for 3 h, washing	D_{H2SO4}
9	Agitation with HCl 3 M for 3 h, washing, heating at 550 °C for 2 h	$D_{HCl+550}$
10	Agitation with H_2SO_4 2.5 M for 3 h, washing, heating at 550 °C for 2 h	$D_{H2SO4+550}$
11	Agitation with HCl 2.5 M for 3 h, washing, stirring with NaOH 3 M for 3 h at 90 °C, washing	$D_{HCl+NaOH}$
12	Agitation with H_2SO_4 2.5 M for 3 h, washing, stirring with NaOH 3 M for 3 h at 90 °C, washing	$D_{H2SO4+NaOH}$
13	Agitation with HCl 2.5 M for 3 h, washing, stirring with NaOH 3 M for 3 h at 90 °C, washing, heating at 550 °C for 2 h	$D_{HCl+NaOH+550}$
14	Agitation with H_2SO_4 2.5 M for 3 h, washing, stirring with NaOH 3 M for 3 h at 90 °C, washing, heating at 550 °C for 2 h	$D_{H2SO4+NaOH+550}$

2.4. Isotherm determination experiments

Isotherm determination experiments were also carried out in 40 mL glass vials with gas-tight caps, non-permeable by organic vapors. Only samples D_{raw}, D_{550}, D_{HCl}, and D_{H2SO4}, which had the highest adsorption capacity, were used in these experiments. Each vial contained the adsorbent in different amounts: 0.01, 0.25, 0.5, 1.0, 1.5, 2.5, 3.5, 4.5 and 5.5 g. Head space within each beaker was minimized, while agitation, contact time (6–24 h, depending on the diatomite sample) and temperature (20 °C) were maintained constant throughout. The solution samples were then filtered (0.45 μm pore filter) and analyzed. Each experiment was carried out at least twice and included a blank sample, in order to determine and take into account any potential contaminant losses due to volatilization. In any case, contaminant losses due to volatilization were determined to be lower than 13%.

2.5. Chemical analysis method

The chemical analysis of the solution samples was performed on a GC-2010 Shimadzu gas chromatographer, coupled to a QP-2010 Plus mass spectrometer, using the Headspace Solid Phase Micro Extraction (HS-SPME) method. The characteristics of the applied method, as determined after proper experimental optimization, were the following:

GC–MS

Injector temperature:	230 °C
Carrier gas:	He
GC column:	SPB^{TM}-1 (15 m × 0.2 mm × 0.2 μm)
Oven temperature:	40 °C for 1 min and increased 5 °C/min up to 60 °C for 0.5 min then increased 30 °C/min up to 270 °C for 2 min
Ion source temperature:	200 °C
GC–MS interface temperature:	280 °C

SPME

Fiber coating:	65 μm polydimethyl siloxane/divinylbenzene (PDMS/DVB)
Sampling mode:	Headspace
Vial volume:	22 mL
Sample volume:	10 mL
Salt addition:	3 g NaCl
Adsorption time:	20 min
Adsorption temperature:	20 °C
Stirring:	1400 rpm
Desorption time:	2 min

Method calibration (internal standard: toluene-d8)

Linear range:	1–12.5 ppb and 0.05–0.75 ppb
Coefficient R^2:	>0.9984 and >0.9972
Limit of Detection:	0.272–0.544 ppb and 0.013–0.028 ppb
Limit of Quantification:	0.906–1.815 ppb and 0.045–0.092 ppb

Matrix effects (tab, lake and sea water)

Relative recoveries:	91–131%

2.6. Matrix and competitive effects

For the determination of any potential matrix effects on the adsorption process of BTEX, MTBE and TAME on diatomite, both kinetic and isotherm experiments were repeated using D_{HCl} and two different aqueous matrices: lake and sea water. The basic physicochemical characteristics of the selected aqueous matrices are shown in Table 2.

For the study of potential competitive effects within the aqueous matrices, three separate solutions containing only one compound out of BTEX, MTBE and TAME were also created and used in kinetic batch experiments.

3. Results and discussion

3.1. Adsorbents characteristics

Raw diatomite presented small specific surface area (BET) (13.04 m^2/g) and micro-pore volume (∼4% of the total pore volume). When treated at relatively low temperatures (250–550 °C), a slight decrease in the BET surface area (from ∼13 down to ∼10 m^2/g) and total pore volume of diatomite was noticed (Table 3). At higher temperatures (>750 °C) the specific surface area of the diatomite significantly decreased (down to 2 m^2/g), indicating important structural changes and possibly a lower potential adsorption capacity. The total pore volume of diatomite decreased at temperatures as high as 1150 °C, due to structural changes caused – supporting similar observations made by Khraisheh et al. [27] and Aivalioti et al. [25].

The chemical treatment and the combination of chemical and thermal treatment of diatomite also caused a reduction in its BET surface area (down to ∼7.5 m^2/g) and its total pore volume.

Fig. 1 represents typical scanning electron micrographs for selected diatomite samples (D_{raw}, D_{HCl}, D_{H2SO4} and D_{550}), showing no great difference between their surface textures.

Table 2
Physicochemical characteristics of the two different aqueous matrices used.

Parameter	Lake water	Sea water
pH	7.76	8.06
Electrical conductivity (μS/cm)	442	57,400
RedOx (mV)	240	168
P (mg/l)	0.09	0.00
Cl^- (mg/l)	14	35,000
NH_4^+ (mg/l)	0.7	2.1
NO_2^- (mg/l)	0.0	0.0
NO_3^- (mg/l)	0.0	0.0
SO_4^{2-} (mg/l)	215	3,200

Table 3
Specific surface area, total pore volume and average pore radius of the diatomite samples.

Sample	Specific surface area, S_{BET} (m^2/g)	Total pore volume (cm^3/g)	Average pore radius (Å)
D_R	13.04	0.02398	73.580
D_{250}	11.36	0.01999	70.384
D_{350}	10.17	0.01398	54.966
D_{550}	10.10	0.01669	66.101
D_{750}	8.68	0.01562	71.986
$D_{1.150}$	2.03	0.00254	50.168
D_{HCl}	9.40	0.01501	63.850
D_{H2SO4}	10.62	0.01664	62.672
$D_{HCl+550}$	9.29	0.01367	58.839
$D_{H2SO4+550}$	9.12	0.01355	59.410
$D_{HCl+NaOH}$	9.06	0.01428	63.014
$D_{H2SO4+NaOH}$	9.40	0.01124	47.815
$D_{HCl+NaOH+550}$	7.78	0.01348	69.303
$D_{H2SO4+NaOH+550}$	7.67	0.01293	67.477

XRD analysis showed that the chemical treatment of the raw diatomite sample, either using acid or base, resulted in the complete removal of any carbonaceous minerals (calcite and aragonite), thereby increasing its purity.

3.2. Adsorption kinetics

The adsorbed moles of selected contaminants per mass of the adsorbate used (mmol g^{-1}) (q_e) in relation to the adsorbent–adsorbate contact time (t in h), for the raw and thermally modified diatomite is presented in Fig. 2, while for the diatomite modified chemically, and both chemically and thermally, is shown in Fig. 3. Given that the kinetic data of the contaminants generally presented the same trend and in order to minimize the number of the provided diagrams, Figs. 2 and 3 include only selected, but representative, contaminants' diagrams.

The adsorption equilibrium time for the raw and thermally treated diatomite was found to be 24 h. This time interval is ten times shorter than that determined for BTEX and MTBE adsorption onto diatomite in a previous study (240 h) [25]. Diatomite treated with HCl presented an even shorter adsorption equilibrium time, equal to 6 h, that remained steady even after any additional treatment of the adsorbent. On the contrary, diatomite treated with H$_2$SO$_4$ presented the same adsorption equilibrium time as the raw and thermally modified diatomite. Only further treatment of this sample, thermal and/or chemical, resulted in a decrease in the adsorption equilibrium time to 12 h. This time period needed for reaching equilibrium is shorter or at least comparable to others
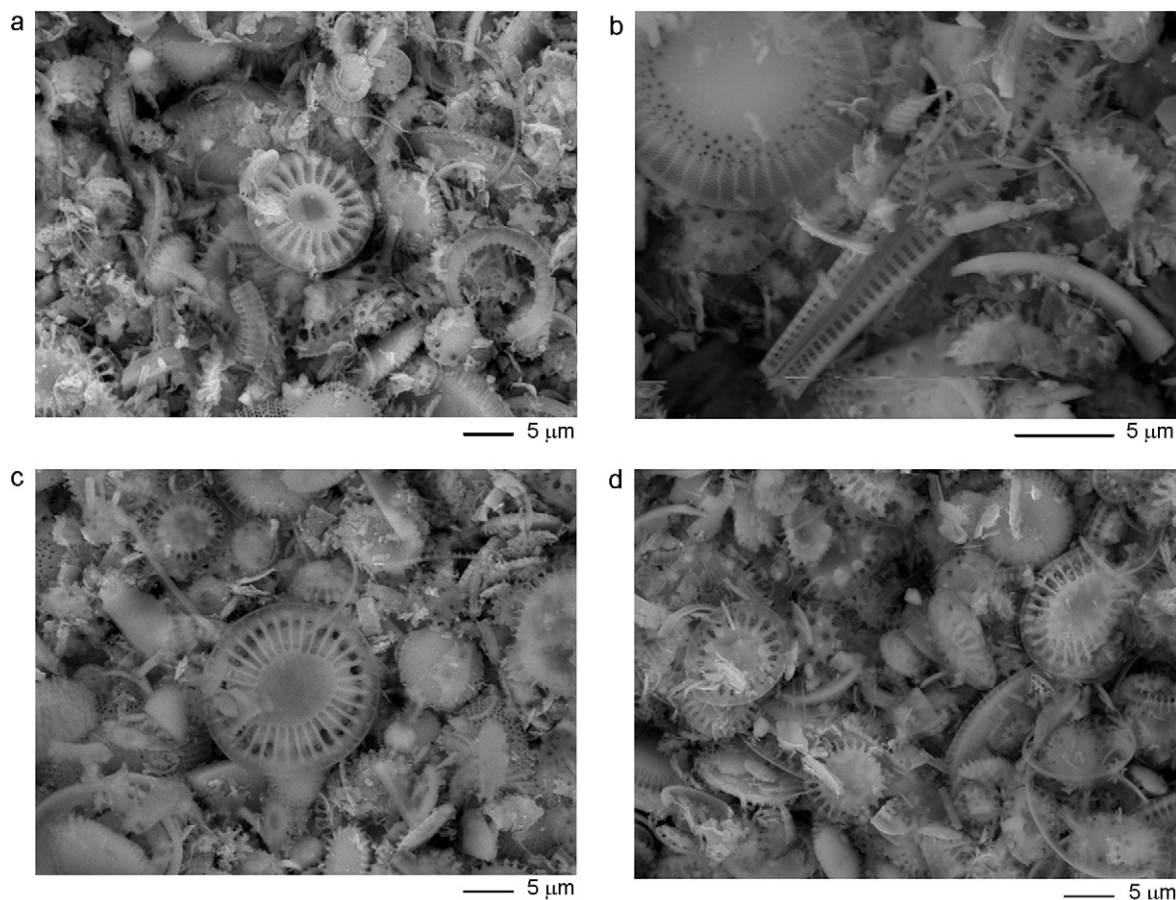

Fig. 1. Typical scanning electron micrographs for (a) D_{raw}, (b) D_{550}, (c) D_{HCl} and (d) D_{H2SO4}.
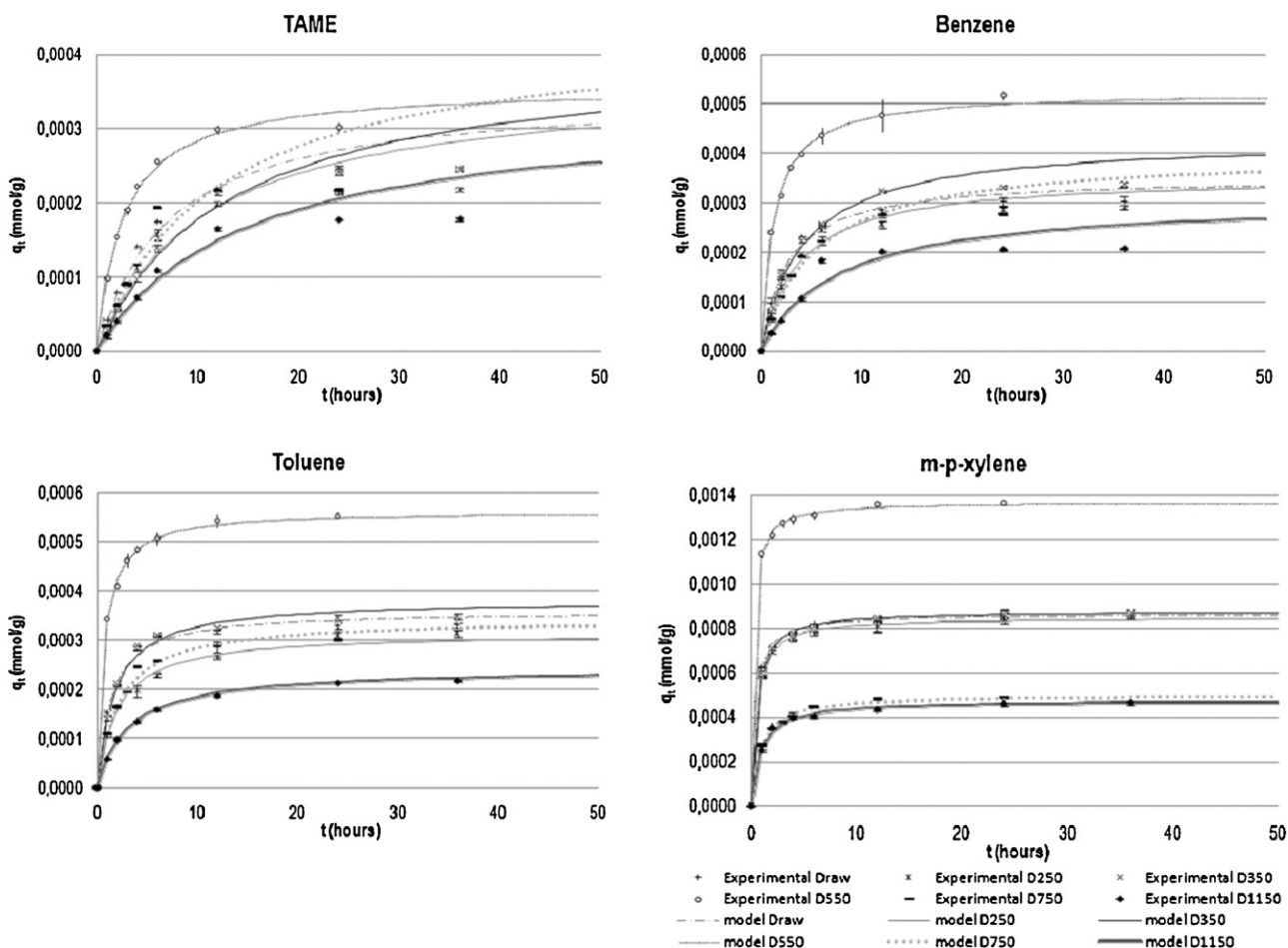
Fig. 2. The adsorbed moles of selected contaminants per mass of the adsorbate used (mmol g^{-1}) (q_e) in relation to the adsorbent–adsorbate contact time (t in h), for the raw and thermally modified diatomite: experimental data and pseudo second order kinetic model fit.

reported for BTEX adsorption on macroreticular resins (10–15 h) [1] and NaOCl-oxidized carbon nanotubes (240 min) [4] and MTBE adsorption on zeolites (10–24 h) [14,15] and resins (≥24 h) [11].

Samples D$_{250}$, D$_{350}$ and D$_{550}$ presented an increasing adsorption capacity, up to ∼125% higher (sample D$_{550}$ – ethylbenzene) than sample D$_{raw}$. On the other hand, samples D$_{750}$ and D$_{1.150}$ presented a significantly lower adsorption capacity, up to ∼46% (sample D$_{1.150}$ – m,p-xylene), compared to that of raw diatomite, probably as a result of the devastating effect that thermal treatment at such high temperatures had on the specific surface area and the micropore area of the diatomite. The chemical treatment of diatomite with acid (whether or not in combination with thermal treatment) increased the material's adsorption capacity for every adsorbate. Sample D$_{HCl}$ presented the maximum adsorption capacity, almost 140% higher than that of D$_{raw}$ (D$_{HCl}$ – ethylbenzene). Fig. 4 illustrates these indicative comparisons of the adsorbed moles of each contaminant per mass of the adsorbate used (mmol g^{-1}) (q_e) for all samples at equilibrium (6–24 h, depending on the sample), under the same experimental conditions ($C = 5$ mg L^{-1} from each contaminant, $m_{adsorbent} = 2$ g, $V_{aq.solut.} = 40$ mL).

As far as the adsorbent preference in the available adsorbates is concerned, it decreases in the following order: m-,p-xylene → o-xylene → ethyl-benzene → toluene → benzene → TAME → MTBE. This order approximately corresponds to the adsorbates' descending order of hydrophobicity (based on their octanol–water coefficient log values), molecular order and ascending order of water solubility. It is confirmed that the most soluble and

hydrophilic substances (TAME and MTBE) have a lesser tendency to adsorb onto the diatomite samples.

In order to interpret the kinetic batch experimental data, three different kinetic models were used: (1) the *pseudo-first-order* kinetic model (Eq. (1)) [33–35], (2) the *pseudo-second-order* kinetic model (Eq. (2)) [34,36,37] and (3) the *intraparticle diffusion model* (Eq. (3)) [21,35].

$$\ln(q_e - q_t) = \ln q_e - k_1 t \tag{1}$$

$$\frac{1}{q_t} = \frac{1}{q_e^2 k_2}\frac{1}{t} + \frac{1}{q_e} \tag{2}$$

$$q_t = x_i + k_p t^{1/2} \tag{3}$$

The value of k_1 was obtained by plotting $\ln(q_e - q_t)$ against t, the value of k_2 was obtained by plotting $1/q_t$ against $1/t$, while the value of k_p was obtained by plotting q_t against $t^{1/2}$.

It became apparent that the kinetics of BTEX, MTBE and TAME adsorption on diatomite followed the pseudo second order model raw diatomite, providing high correlation coefficient (R^2) values ranging from 0.9812 (sample D$_{1150}$ – m,p-xylene) up to 0.9992 (sample D$_{1550}$ – ethylbenzene).

The values of the pseudo-second order rate constants k_2 and q_e for selected diatomite samples are presented in Table 4. Clearly, the thermal treatment of diatomite at 550 °C not only increased the adsorption capacity of the material, but also accelerated the adsorption kinetic rate for all the examined adsorbates. Likewise, the chemical treatment of diatomite with HCl further increased both the adsorption capacity and the kinetic rate. Given that
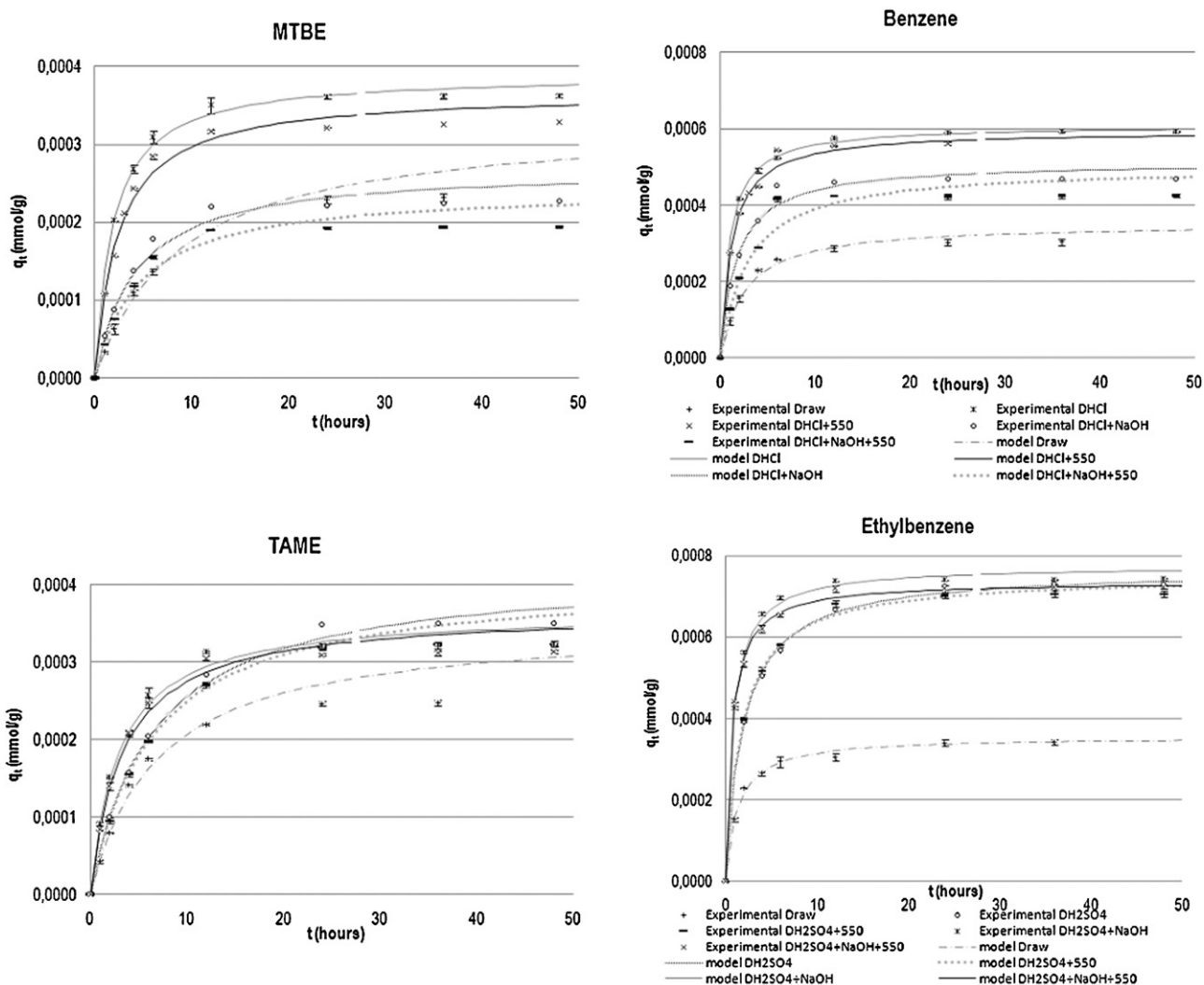
Fig. 3. The adsorbed moles of selected contaminants per mass of the adsorbate used (mmol g^{-1}) (q_e) in relation to the adsorbent–adsorbate contact time (t in h), for the raw and chemically and both chemically and thermally modified diatomite experimental data and pseudo second order kinetic model fit.

D$_{550}$ has a slightly larger specific surface area than D$_{HCl}$, this fact can only be attributed to the modified mineralogical composition and surface properties, caused by the acid treatment of the diatomite.

3.3. Adsorption isotherms

The adsorbed moles of selected contaminants per mass of the adsorbate used (mmol g^{-1}) (q_e) in relation to the adsorbate con-
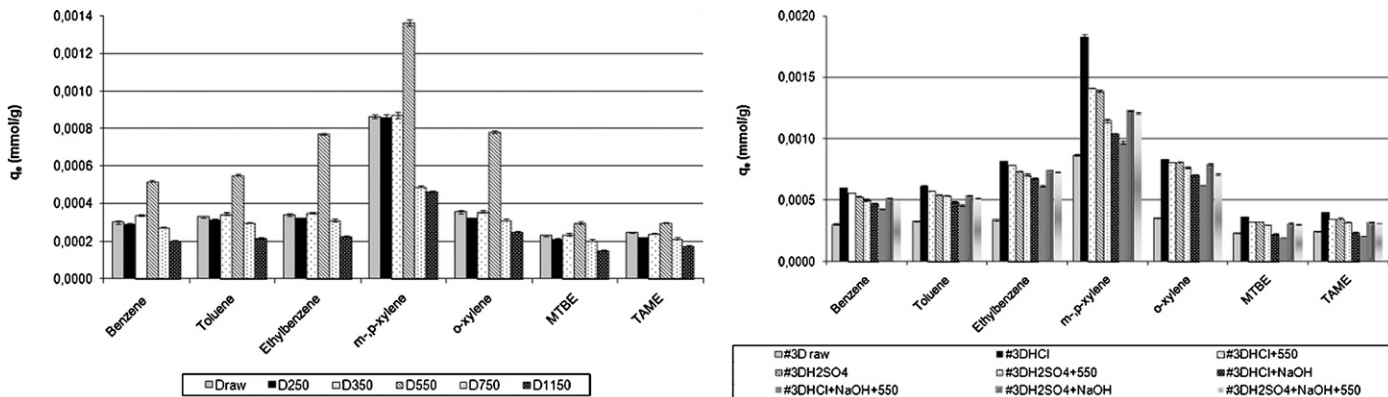

Fig. 4. Indicative comparison of the adsorbed moles of each contaminant per mass of the adsorbate used (mmol g^{-1}) (q_e) for all samples at equilibrium (6–24 h, depending on the sample) ($C = 5$ mg L^{-1} from each contaminant, $m_{adsorbent} = 2$ g).
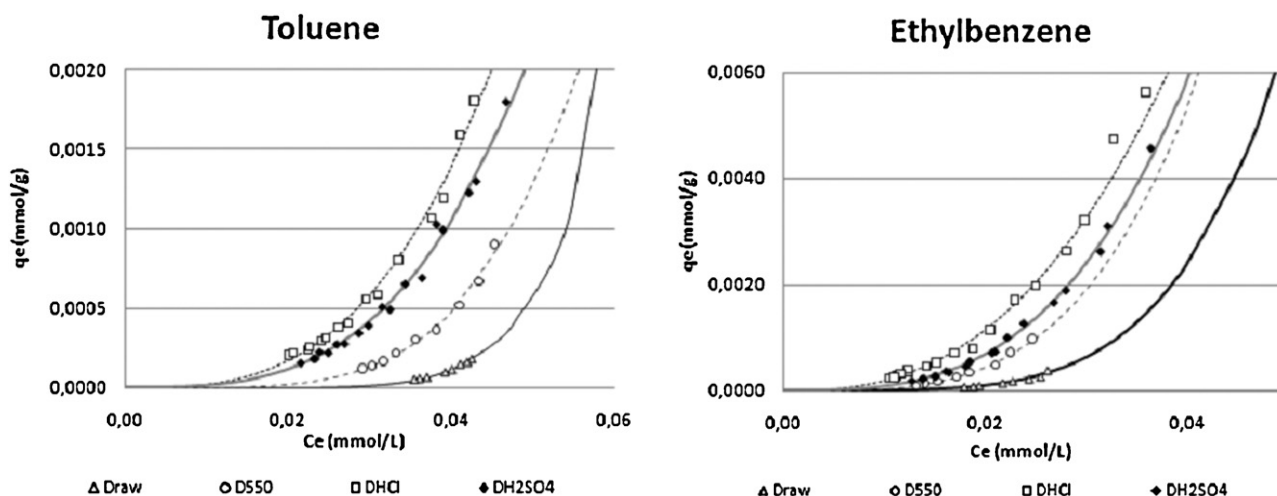
Fig. 5. The adsorbed moles of selected contaminants per mass of the adsorbate used (mmol g^{-1}) (q_e) in relation to the adsorbate concentration in the aqueous phase (C in mmol/L) for all diatomite samples D_{raw}, D_{550}, D_{HCl} and D_{H2SO4}: experimental data and Freundlich isotherm model fit.

centration in the aqueous phase (C in mmol/L) for all diatomite samples D_{raw}, D_{550}, D_{HCl} and D_{H2SO4} are presented in Fig. 5.

The Freundlich model best fitted the experimental data for each one of the examined diatomite samples and the selected adsorbates, based on the high values of correlation coefficient R^2 that varied from 0.9839 (sample D_{raw} – TAME) to 0.9984 (sample D_{raw} – o-xylene) (Table 5). On the contrary, the other two examined isotherm models presented significantly lower values of the correlation coefficient R^2 for every adsorbate and poor fit to the experimental data.

The Freundlich constant $1/n$ was calculated to be greater than unity for every diatomite sample and every adsorbate, indicating unfavorable adsorption. However, both thermal and chemical treatment favored the contaminants' adsorption on diatomite, as it is indicated by the decreased values of $1/n$ for samples D_{550}, D_{HCl} and D_{H2SO4}, compared to sample D_{raw}.

3.4. Matrix effects

When lake and sea water were used as the aqueous matrix of the contaminant solutions, the adsorption equilibrium time for sample D_{HCl} was again 6 h (Fig. 6). However, its adsorption capacity was significantly lower (up to 50% less) than that obtained when distilled water was the aqueous matrix (Fig. 7). Evidently the intrinsic components of natural water greatly influence the adsorption process of BTEX, MTBE and TAME on diatomite. This influence must be taken

Table 4
Results of the pseudo second order model fits for selected experimental data.

Adsorbate	Pseudo second order model		
	q_e (mmol g^{-1})	k_2 (g mmol^{-1} h^{-1})	R^2
D_{raw}			
MTBE	0.0003	343.32	0.9975
Benzene	0.0004	1104.84	0.9936
TAME	0.0004	410.84	0.9951
Toluene	0.0004	2100.44	0.9897
Ethyl-benzene	0.0004	2171.53	0.9893
m-,p-Xylene	0.0009	2915.27	0.9950
o-Xylene	0.0004	2345.33	0.9949
D_{550}			
MTBE	0.0004	987.23	0.9964
Benzene	0.0005	1583.98	0.9937
TAME	0.0004	1077.05	0.9978
Toluene	0.0006	2699.25	0.9910
Ethyl-benzene	0.0008	3209.60	0.9850
m-,p-Xylene	0.0014	3426.74	0.9854
o-Xylene	0.0008	3312.80	0.9837
D_{HCl}			
MTBE	0.0004	1410.51	0.9898
Benzene	0.0006	1773.31	0.9961
TAME	0.0004	1445.08	0.9864
Toluene	0.0006	2818.56	0.9923
Ethyl-benzene	0.0008	3257.52	0.9962
m-,p-Xylene	0.0018	3595.16	0.9879
o-Xylene	0.0008	3415.06	0.9833

Table 5
Results of the Freundlich fits for selected experimental data.

| Sample	Freundlich isotherm		
	k_F (mmol g^{-1} (L mmol^{-1})$^{-1/n}$)	$1/n$	R^2
MTBE			
D_{raw}	3.365E+13	15.1240	0.9976
D_{550}	1.553E+03	6.6116	0.9934
D_{H2SO4}	2.508E+01	4.5279	0.9923
D_{HCl}	1.149E+02	4.8021	0.9961
Benzene			
D_{raw}	6.797E+0.5	7.7534	0.9965
D_{550}	1.442E+03	5.3006	0.9842
D_{H2SO4}	3.395E+01	3.6105	0.9879
D_{HCl}	2.213E+01	3.3271	0.9918
TAME			
D_{raw}	4.688E+11	11.6810	0.9839
D_{550}	9.207E+03	5.7246	0.9908
D_{H2SO4}	4.958E+02	4.6218	0.9944
D_{HCl}	6.108E+02	4.5570	0.9972
Toluene			
D_{raw}	2.289E+06	7.7205	0.9948
D_{550}	7.532E+02	4.4316	0.9958
D_{H2SO4}	2.956E+01	3.1854	0.9926
D_{HCl}	2.160E+01	2.9970	0.9918
Ethylbenzene			
D_{raw}	7.672E+03	4.6547	0.9866
D_{550}	5.206E+02	3.5682	0.9927
D_{H2SO4}	1.240E+02	3.0964	0.9970
D_{HCl}	2.484E+01	2.5485	0.9927
m-,p-Xylene			
D_{raw}	2.698E+01	3.8517	0.9941
D_{550}	3.282E−01	2.0616	0.9945
D_{H2SO4}	1.096E+00	2.4102	0.9973
D_{HCl}	1.628E+00	2.4125	0.9925
o-Xylene			
D_{raw}	3.031E+02	3.9254	0.9984
D_{550}	4.296E+01	3.1194	0.9960
D_{H2SO4}	5.868E+00	2.5097	0.9921
D_{HCl}	1.554E+01	2.7287	0.9902
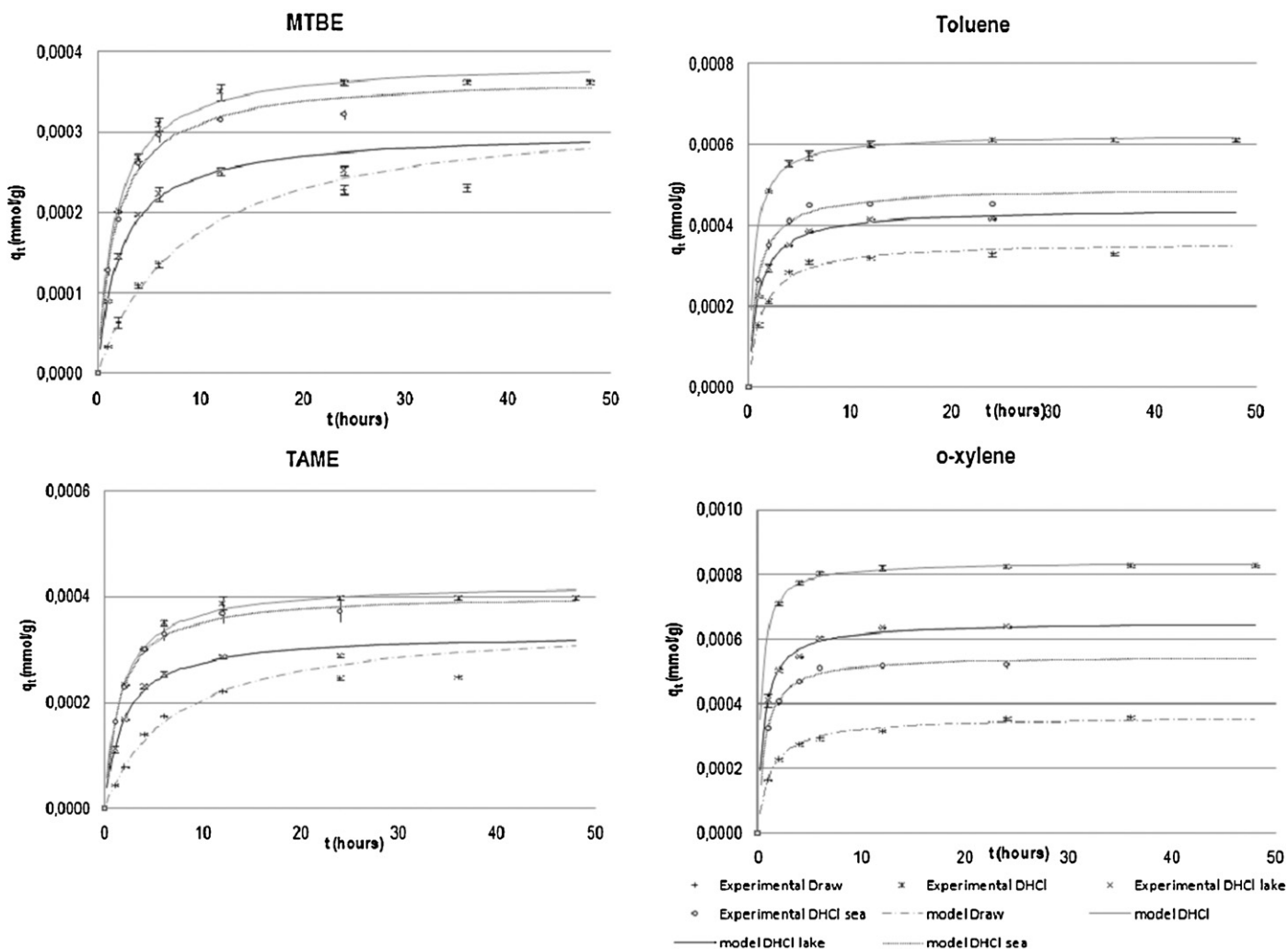
Fig. 6. The adsorbed moles of selected contaminants per mass of the adsorbate used (mmol g^{-1}) (q_e) in relation to the adsorbent–adsorbate contact time (t in h), for D$_{HCl}$, in different aqueous matrices (sea and lake).

into account and quantified when diatomite – BTEX + MTBE + TAME adsorption systems are to be designed, in order to avoid any future failures.

It is important to point out that the adsorption capacity q_e of both MTBE and TAME did not decrease in the sea water as much as it did in the lake water (Fig. 7). This can be attributed to the relatively high polarity of MTBE and TAME, compared to that of
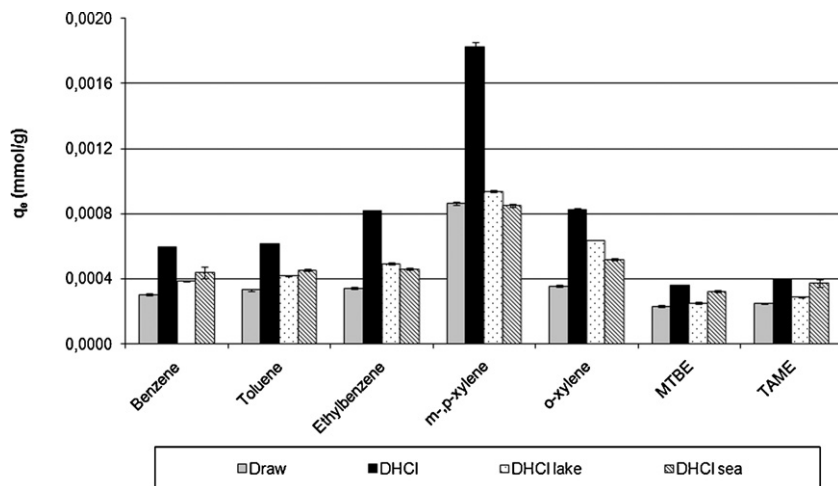

Fig. 7. Indicative comparison of the adsorbed moles of each contaminant per mass of the adsorbate used (mmol g^{-1}) (q_e) after equilibrium was reached, during the matrix effects experiments.

Table 6
Results of the pseudo second order model fits for the matrix and competitive effects experiments.

Adsorbate	Pseudo second order model		
	q_e (mmol g^{-1})	k_2 (g mmol^{-1} h^{-1})	R^2
D$_{HCl\ lake}$			
MTBE	0.0003	1461.58	0.9937
Benzene	0.0004	2256.29	0.9902
TAME	0.0003	1586.00	0.9970
Toluene	0.0004	2346.48	0.9983
Ethyl-benzene	0.0005	2441.96	0.9874
m-,p-Xylene	0.0010	2780.23	0.9852
o-Xylene	0.0007	2589.16	0.9866
D$_{HCl\ sea}$			
MTBE	0.0004	1472.30	0.9951
Benzene	0.0005	2308.47	0.9936
TAME	0.0004	1669.74	0.9975
Toluene	0.0005	2445.95	0.9880
Ethyl-benzene	0.0005	2481.16	0.9927
m-,p-Xylene	0.0009	2738.26	0.9913
o-Xylene	0.0005	2714.10	0.9931
D$_{HCl\ lake\ BTEX}$			
Benzene	0.0004	2080.13	0.9948
Toluene	0.0005	2149.9	0.9939
Ethyl-benzene	0.0006	2365.49	0.9893
m-,p-Xylene	0.0009	2576.50	0.9887
o-Xylene	0.0007	2425.26	0.9980
D$_{HCl\ lake\ MTBE+TAME}$			
MTBE	0.0006	2111.52	0.9911
TAME	0.0006	2440.52	0.9908
D$_{HCl\ sea\ BTEX}$			
Benzene	0.0005	2241.18	0.9959
Toluene	0.0005	2407.86	0.9991
Ethyl-benzene	0.0005	2712.88	0.9917
m-,p-Xylene	0.0009	3397.18	0.9877
o-Xylene	0.0006	2908.63	0.9901
D$_{HCl\ sea\ MTBE+TAME}$			
MTBE	0.0008	2167.79	0.9930
TAME	0.0009	2359.25	0.9966

Table 7
Results of the Freundlich fits for the matrix effects experiments.

Sample	Freundlich isotherm		
	k_F (mmol g^{-1} (L mmol^{-1})$^{-1/n}$)	$1/n$	R^2
MTBE			
D$_{HCl\ lake}$	5.761E+01	5.1221	0.9812
D$_{HCl\ sea}$	5.420E+00	3.8890	0.9830
Benzene			
D$_{HCl\ lake}$	1.367E+02	4.5081	0.9925
D$_{HCl\ sea}$	5.761E+02	5.0747	0.9843
TAME			
D$_{HCl\ lake}$	1.346E+03	5.0943	0.9945
D$_{HCl\ sea}$	2.925E+01	3.6610	0.9964
Toluene			
D$_{HCl\ lake}$	9.676E+01	4.0127	0.9958
D$_{HCl\ sea}$	4.372E+02	4.3875	0.9896
Ethylbenzene			
D$_{HCl\ lake}$	6.524E+02	3.9016	0.9926
D$_{HCl\ sea}$	1.567E+03	4.2238	0.9954
m-,p-Xylene			
D$_{HCl\ lake}$	2.66E+00	3.0810	0.9901
D$_{HCl\ sea}$	3.827E+00	3.1254	0.9908
o-Xylene			
D$_{HCl\ lake}$	1.068E+01	3.1351	0.9867
D$_{HCl\ sea}$	2.211E+02	4.0478	0.9866

contaminants per mass of the adsorbate used (mmol g^{-1}) (q_e) in relation to the adsorbate concentration in the aqueous phase (C in mmol/L) for diatomite sample D$_{HCl}$ and all matrices (ultrapure, lake and sea water) are presented in Fig. 8.

3.5. Competitive effects

The presence of BTEX in an aqueous solution significantly forestalled both MTBE and TAME adsorption onto diatomite (D$_{HCl}$) (Fig. 9). More specifically, in the lake water, when MTBE and TAME were the sole adsorbates present, their adsorption onto D$_{HCl}$ was almost 2.0 and 1.9 times higher, respectively, than when BTEX co-existed in the aqueous solution. In the sea water, the relevant adsorptions were about 2.3 and 2.4 times higher, respectively.

BTEX was clearly preferred by the adsorbent used in this study, against MTBE and TAME which were the contaminants with the lowest adsorption tendency. In fact MTBE and TAME presence in the solution did not really influence BTEX adsorption onto D$_{HCl}$ (Fig. 9). BTEX presented a higher adsorption tendency on diatomite, due to their physical properties (e.g. less solubility), rapidly covering the vast available surface of the adsorbent. BTEX's lower solubility in water, as well as its higher hydrophobia, compared to that of TAME and MTBE, also promoted and accelerated BTEX adsorption onto the adsorbent.
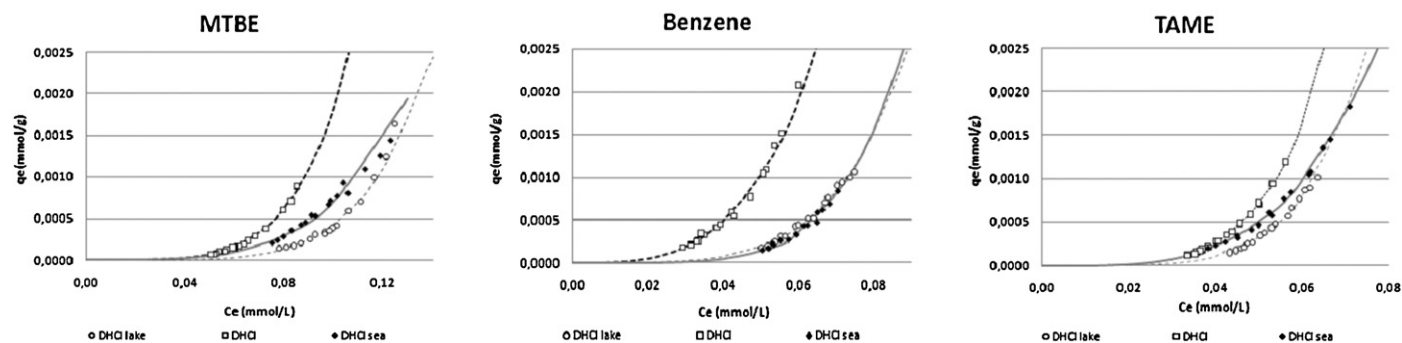
BTEX, which results in a matrix of high ionic strength (sea water) having a strong effect on their extraction from the aqueous phase and consequently on their adsorption onto diatomite.

The adsorption kinetics changed when natural water was used as an aqueous matrix, but still the pseudo second order model best fitted the experimental data, providing high correlation coefficient (R^2) values ranging from 0.9852 (m-p-xylene – lake water) up to 0.9983 (toluene – lake water) (Table 6). The constant rate k_2 values increased for benzene, MTBE and TAME when natural water was used, while for all the other adsorbates it decreased.

The Freundlich isotherm again gave a best fit to the experimental data (Table 7). The Freundlich constant $1/n$ values were slightly higher than those calculated when ultrapure water was used, with the exception of MTBE and TAME in the sea water, for which lower $1/n$ values were recorded. The adsorbed moles of selected

Fig. 8. The adsorbed moles of selected contaminants per mass of the adsorbate used (mmol g^{-1}) (q_e) in relation to the adsorbate concentration in the aqueous phase (C in mmol/L) for D$_{HCl}$, in different aqueous matrices (sea and lake): experimental data and Freundlich isotherm model fit.
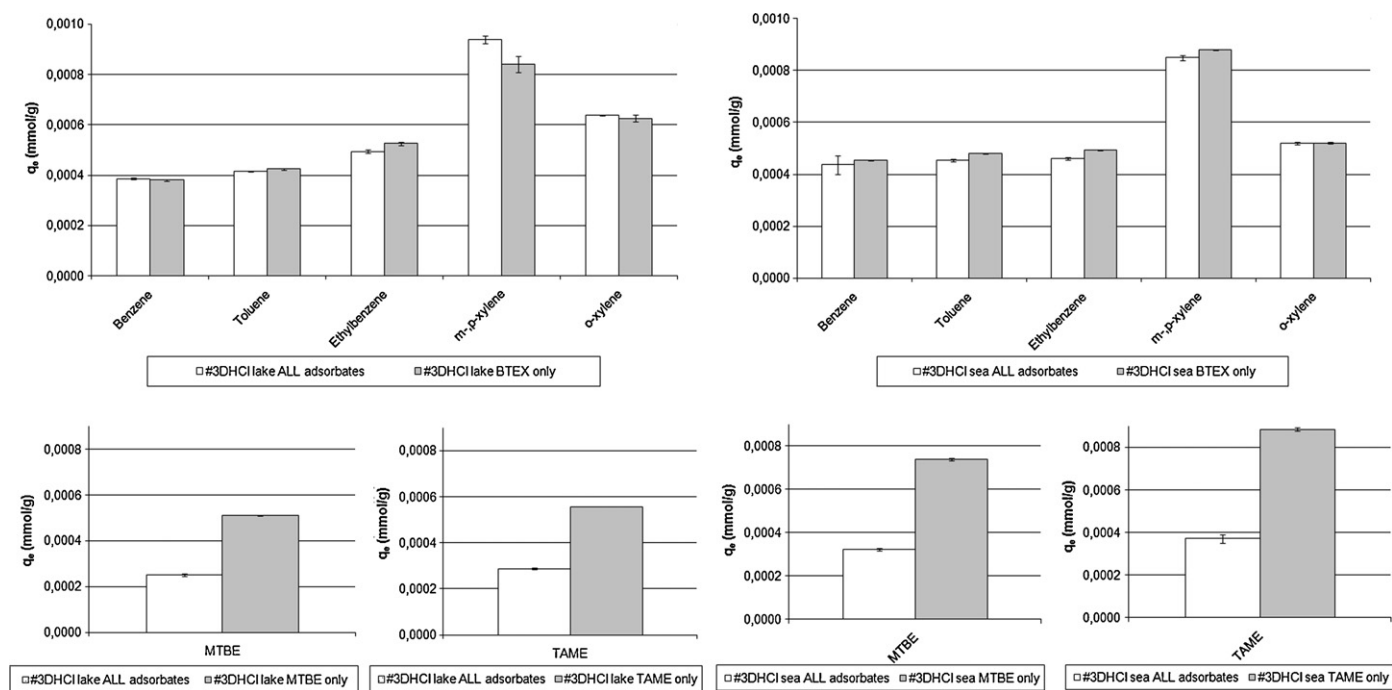
Fig. 9. Indicative comparison of the adsorbed moles of each contaminant per mass of the adsorbate used $(\mathrm{mmol\,g^{-1}})$ (q_e) after equilibrium was reached, during the competitive effects experiments.

The pseudo second order model rate k_2 values increased for the sole adsorbents only in the case of MTBE and TAME, up to as much as 54% (Table 6).

4. Conclusions

The goal of this paper was to explore and present diatomite's capacity to adsorb certain common petroleum contaminants. Therefore raw diatomite, as well as diatomite that was treated thermally, chemically and both thermally and chemically, were used for the adsorption of BTEX, MTBE and TAME from aqueous solutions. Finally, the following major conclusions were drawn:

- The thermal and/or chemical treatment of diatomite generally results in small changes in its specific surface area, with the exception of thermal treatment at high temperatures (>750 °C) that causes severe destruction of micropores and a dynamic decrease in the specific surface area of the material.
- Adsorption equilibrium is reached between 6 and 24 h, depending on the diatomite pre-treatment; a period that can still be considered quite short (at least for in situ applications, such as permeable reactive barriers).
- Diatomite treated with HCl presents the highest adsorption capacity for the examined contaminants and the shortest adsorption equilibrium time (6 h).
- The adsorbent preference in the available adsorbates decreases in the following order: m-,p-xylene → o-xylene → ethylbenzene → toluene → benzene → TAME → MTBE. As a result, the presence of BTEX significantly reduces MTBE and TAME adsorption onto diatomite, due to competitive effects.
- The use of natural water (sea and lake) as the aqueous matrix instead of distilled water results in a substantial decrease in the adsorption capacity of the diatomite, indicating that the intrinsic components of natural water greatly influence the adsorption process. This fact must always be taken into account when adsorption processes are studied and relevant systems are designed.

- The pseudo second order kinetics model best describes the kinetics of BTEX, MTBE and TAME adsorption onto diatomite.
- The Freundlich model best fits the isotherm experimental data, providing $1/n$ values greater than one (unfavorable adsorption).

References

[1] H.S. Lin, Y.C. Huang, Adsorption of BTEX from aqueous solution by macroreticular resins, J. Hazard. Mater. A 70 (1999) 21–37.
[2] J.A. Simpsona, R.S. Bowman, Nonequilibrium sorption and transport of volatile petroleum hydrocarbons in surfactant-modified zeolite, J. Contam. Hydrol. 108 (1–2) (2009) 1–11.
[3] O. Carmody, R. Frost, Y. Xi, S. Kokot, Adsorption of hydrocarbons on organoclays – implications for oil spill remediation, J. Colloid Interf. Sci. 305 (2007) 17–24.
[4] F. Su, C. Lu, S. Hu, Adsorption of benzene, toluene, ethylbenzene and p-xylene by NaOCl-oxidized carbon nanotubes, Colloid Surf. A: Physicochem. Eng. Aspects 353 (2010) 83–91.
[5] C. Lu, F. Su, S. Hu, Surface modification of carbon nanotubes for enhancing BTEX adsorption from aqueous solutions, Appl. Surf. Sci. 254 (2008) 7035–7041.
[6] B. Ji, F. Shao, G. Hu, S. Zheng, Q. Zhang, Z. Xu, Adsorption of methyl tert-butyl ether (MTBE) from aqueous solution by porous polymeric adsorbents, J. Hazard. Mater. 161 (2009) 81–87.
[7] A.O. Yazaydin, W.R. Thompson, Molecular simulation of the adsorption of MTBE in silicate, mordenite and zeolite beta, J. Phys. Chem. 110 (2006) 14458–14462.
[8] M.C. Annesini, F. Gironi, B. Monticelli, Removal of oxygenated pollutants from wastewater by polymeric resins: data on adsorption equilibrium and kinetics in fixed beds, Water Res. 34 (2000) 2989–2996.
[9] E. Bi, S. Haderlein, T. Schmidt, Sorption of methyl tert-butyl ether (MTBE) and tert-butyl alcohol (TBE) to synthetic resins, Water Res. 39 (2005) 4164–4176.
[10] H. Hung, T. Lin, Adsorption of MTBE from contaminated water by carbonaceous resins and mordenite zeolite, J. Hazard. Mater. 135 (2006) 210–217.
[11] B. Burghoff, J.S. Marques, B.M. Van Lankvelt, A.B. De Haan, Solvent impregnated resins for MTBE removal from aqueous environments, React. Funct. Polym. 70 (2010) 41–47.
[12] M.A. Anderson, Removal of MTBE and other organic contaminants from water by sorption to high silica zeolites, Environ. Sci. Technol. 34 (2000) 725–727.

[13] D.R.U. Knappe, A.A.R. Campos, Effectiveness of high-silica zeolites for the adsorption of methyl tertiary-butyl ether from natural water, Water Sci. Technol.: Water Supply 5 (5) (2005) 83–91.

[14] L. Abu-Lail, J.A. Bergendahl, R.W. Thompson, Adsorption of methyl tertiary butyl ether on granular zeolites: batch and column studies, J. Hazard. Mater. 178 (2010) 363–369.

[15] J. Lu, F. Xu, D. Wang, J. Huang, W. Cai, The application of silicate-1/fly ash cenosphere (S/FAC) zeolite composite for the adsorption of methyl tert-butyl ether (MTBE), J. Hazard. Mater. 165 (2009) 120–125.

[16] L. Yu1, C. Adams, D. Ludlow, Adsorption isotherms for methyl tert-butyl ether and other fuel oxygenates on two bituminous-coal activated carbons, J. Environ. Eng. 131 (6) (2005) 983–987.

[17] C.D. Adams, J. Sutherland, J. Kekobad, Comparative treatment study of MTBE and alternative fuel oxygenates – final report, December 2002, University of Missouri-Rolla.

[18] H. Arik, Synthesis of Si_3N_4 by the carbo-thermal reduction and nitridation of diatomite, J. Eur. Ceram. Soc. 23 (2003) 2005–2014.

[19] S. Akin, J.M. Schembre, S.K. Bhat, A.R. Rovscek, Spontaneous imbibition characteristics of diatomite, J. Petrol. Sci. Eng. 25 (2000) 149–165.

[20] B.T. Hoffman, A.R. Kovscek, Displacement front stability of steam injection into high porosity diatomite rock, J. Petrol. Sci. Eng. 46 (2005) 253–266.

[21] M. Al-Ghouti, M.A.M. Khraisheh, M.N.M. Ahmad, S. Allen, Thermodynamic behaviour and the effect of temperature on the removal of dyes from aqueous solution using modified diatomite: a kinetic study, J. Colloid Interf. Sci. 287 (2005) 6–13.

[22] B. Gao, P. Jiang, F. An, S. Zhao, Z. Ge, Studies on the surface modification of diatomite with polyethyleneimine and trapping effect of the modified diatomite for phenol, Appl. Surf. Sci. 250 (2005) 273–279.

[23] O. Şan, R. Gören, C. Özgür, Pyrification of diatomite powder by acid leaching for use in fabrication of porous ceramics, Int. J. Miner. Process. 93 (2009) 6–10.

[24] P. Yuan, D.Q. Wu, H.P. He, Z.Y. Lin, The hydroxyl species and acid sites on diatomite surface: a combined IR and Raman study, Appl. Surf. Sci. 227 (2004) 30–39.

[25] M. Aivalioti, I. Vamvasakis, E. Gidarakos, BTEX and MTBE adsorption onto raw and thermally modified diatomite, J. Hazard. Mater. 178 (1–3) (2010) 136–143.

[26] P. Yuan, D. Yang, Z. Lin, H. He, X. Wen, L. Wang, F. Deng, Influences of pretreatment temperature on the surface silylation of diatomaceous amorphous silica with thimethylchlorosilane, J. Non-Cryst. Solids 352 (2006) 3762–3771.

[27] M.A.M. Khraisheh, M.A. Al-Ghouti, S.J. Ghouti, S.J. Allen, M.N. Ahmad, Effect of OH and silanol groups in the removal of dyes from aqueous solution using diatomite, Water Res. 39 (2005) 922–932.

[28] W. Xiong, J. Peng, Development and characterization of ferrihydrite-modified diatomite as a phosphorus adsorbent, Water Res. 42 (2008) 4869–4877.

[29] W.T. Tsai, K.J. Hsien, J.M. Yang, Silica adsorbent prepared from spent diatomaceous earth and its application to removal of dye from aqueous solution, J. Colloid Interf. Sci. 275 (2004) 428–433.

[30] A. Chaisena, K. Rangariwatananon, Synthesis of sodium zeolites from natural and modified diatomite, Mater. Lett. 59 (2005) 1474–1479.

[31] E. Galàn, I. González, E. Mayoral, A. Miras, Properties and applications of diatomitic materials from SW Spain, Appl. Clay Sci. 8 (1993) 1–18.

[32] P. Huttenloch, K.E. Roehl, K. Czurda, Sorption of nonpolar aromatic contaminants by chlorosilane surface modified natural minerals, Environ. Sci. Technol. 35 (2001) 4260–4264.

[33] R.A. Shawabkeh, M.F. Tununji, Experimental study and modeling of basic dye sorption by diatomaceous clay, Appl. Clay Sci. 24 (2003) 111–120.

[34] Z. Al-Qodah, W.K. Lafi, Z. Al-Anber, M. Al-Shannag, A. Harahsheh, Adsorption of methylene blue by acid and heat treated diatomaceous silica, Desalination 217 (2007) 212–224.

[35] A.A.M. Daifullah, B.S. Girgis, Impact of surface characteristics of activated carbon on adsorption of BTEX, Colloid Surf. A 214 (2003) 181–193.

[36] W.T. Tsai, K.J. Hsien, Y.M. Chang, C.C. Lo, Removal of herbicide paraquat from an aqueous solution by adsorption onto spent and treated diatomaceous earth, Bioresour. Technol. 96 (2005) 657–663.

[37] W.T. Tsai, C.W. Lai, T.Y. Su, Adsorption of bisphenol-A from aqueous solution onto minerals and carbon adsorbents, J. Hazard. Mater. B 134 (2006) 169–175.